CrossMark

TECHNICAL PAPER

Free vibration and critical angular velocity of a rotating variable thickness two-directional FG circular microplate

M. H. Shojaeefard[1] · H. Saeidi Googarchin[2] · M. Mahinzare[2] · M. Ghadiri[3]

Abstract In this paper, the free vibration of a rotating variable thickness two-directional FG circular microplate is studied. The governing equations of motion for the microplate are extracted utilizing the Hamiltonian's principle in conjunction with the first shear deformation theory as well as the modified couple stress theory. The solution of equations is presented utilizing the differential quadrature method. In special cases, the natural frequency results obtained by the reduced form of the proposed formulation are compared with those available in the literature, indicating a very good accuracy. The results reveal that there is a non-proportional relation between the natural frequencies of the microplate and the thickness-variations of the section. In contrast, the critical angular velocity of that is not much sensitive with respect to the thickness variation. Moreover, the analyses indicate the significant impact of the two-directionality-variation of the graded material on the natural frequencies as well as the critical angular velocities. A map on the effects of the two-directionality-variation of the material property on the free vibration of the microplate is presented. The results show that the increase of the size dependency would lead to the reduction of the non-dimensional natural frequency as well as the critical angular velocity.

1 Introduction

The increasing demands for the structures bearing the higher mechanical and thermal load lead to introduce the advanced composite structures like functionally graded materials (FGM) in industry. In comparison with competitive materials, the higher strength to weight ratio and the reduction of the delamination failure are the significant advantages that result in the more application of FGM beams, plates and shell in industry. While the FGMs are comprehensively used in macro- micro- and nano-sizes, the tradition applications are limited to those structures that are subjected to thermal and mechanical loads varying in thickness direction only. Since the multi-axial loading on the structures is the frequent ones that are inevitable. In this way, recently, multi-directional FGMs are introduced to use in such structures. In addition, the thickness variability enables the designer to reach the most efficient structures. Since there are many investigations about static (Ghadiri and Shafiei 2015; Salamat-Talab et al. 2012; Eshraghi et al. 2016; Ansari et al. 2015; Duan and Wang 2007; Kadkhodayan and Golmakani 2014; Ma and Wang 2003; Chaht et al. 2015), buckling (Van and Hoa 2013; Jabbari et al. 2014; Bedroud et al. 2013; Mehri et al. 2016; Jin et al. 2014; Özakça et al. 2003; Anjomshoa 2013; Wang et al. 2006; Farajpour et al. 2012; Tsiatas and Yiotis 2014; Gholami et al. 2015, 2016) and vibration (Şimşek and Kocatürk 2009; Wei et al. 2012; Şimşek and Reddy 2013; Huang et al. 2013; Huang and Li 2010; Alshorbagy et al. 2011; Shahba and Rajasekaran 2012; Shahba et al. 2011; Neves et al. 2012a, b, 2013; Şimşek et al. 2012; Aydogdu and Taskin

✉ H. Saeidi Googarchin
 hsaeidi@iust.ac.ir

 M. Mahinzare
 mohammadmahinzare@gmail.com

[1] Mechanical Engineering Department, Iran University of Science and Technology, Tehran 16846-13114, Iran

[2] Automotive Fluids and Structures Analysis Research Laboratory, School of Automotive Engineering, Iran University of Science and Technology, Tehran 16846-13114, Iran

[3] Department of Mechanics, Faculty of Engineering, Imam Khomeini International University, Qazvin 34149-16818, Iran

2007; Şimşek 2010a, b; Khalili et al. 2010; Akgöz and Civalek 2013; Şimşek 2012; Pradhan and Chakraverty 2013; Ghadiri et al. 2015; Ebrahimi et al. 2015; Ghadiri and Hosseini 2014; Shafiei et al. 2016a, b, c, d; Ghadiri and Shafiei 2016a, b; Ghadiri et al. 2016) of one-directional FGMs, the shortcoming of studies on the variable thickness multi-directional FGMs could be seen in the literature. The rarely available studies are only limited to macro-size structures (i.e. beams, plates and shells).

Shariyat and Alipour (2013) and Shariyat et al. (2013) developed a power series solution for the free vibration and the damping analyses of a viscoelastic functionally graded plate with a variable thickness on the elastic foundation. Moreover, Alipour and Shariyat (2013) presented a semi-analytical solution for the buckling analysis of a two-directional FG circular plate with a variable thickness on the elastic foundation. Satouri (2015) studied the free vibration of a two-directional FG sectorial plate with a variable thickness resting on a Winkler–Pasternak elastic foundation. Alinaghizadeh and Shariati (2015, 2016) investigated the static bending of two-directional FG circular/annular sector plates with a variable thickness.

While some investigations were conducted on the macro-size structures, as the best knowledge of the authors, there is not any investigation about the free vibration of a two-directional FG micro-structure with a variable thickness.

In this study, the governing equations of motion for a rotating variable thickness two-directional FG circular microplate are developed considering the modified couple stress. The vibration solution of the equations is presented using differential quadrature method (DQM). In special cases, the results are verified with the available results in the literature. The contributions of size dependency, two-directionality-variation of FG material and thickness variation effects on the first natural frequencies of a micro-plate are studied. The novelty of this study could be summarized as follows:

- The presentation of a formulation for a circular plate considering a variable thickness for the section and a two-directional FG for the material as well as a rotating velocity for the structure, all in the micro-size.
- A parametric study on the contributions of the thickness-variation in the section, two-directionality-variation in the material property and the rotating velocity of the microplate on the natural frequencies as well as the critical angular velocities of a circular microstructure.

2 Formulation

In this section, material assumptions and governing equations of motion in conjunction with associated boundary conditions utilizing first shear deformation theories are

presented. Since formulation is derived for a variable thickness two-directional FG circular microplate under rotational velocity condition, the governing equations are enriched with the modified couple stress effects.

2.1 Material

A schematic of a variable thickness two-directional FG circular microplate is represented in Fig. 1. As can be seen in Fig. 1, h_0 and R are the central thickness and the outer radius of the microplate, respectively. The thickness is the maximum in the central point and there is a reduction for the thickness in the radial-direction. It is assumed that the microplate made from a combination of metal and ceramic. The combination changes from the top to the bottom surface of the plate as well as from the center to the outer radius of plates, i.e. the top surface of the plate in central point of the plate ($z = h_0/2$, $r = 0$) is ceramic-rich whiles the bottom surface of the plate in central point of the plate ($z = -h_0/2$, $r = 0$) is metal-rich. The angular velocity of the rotating microplate is equal with Ω.

Therefore, a two-directional functionally graded material (FGM) character, P, of the circular plate is assumed to vary through the thickness and radius respected to the volume fraction of the constituent components, V_i, as follows (Shariyat and Alipour 2013):

$$P(r,z) = (P_t V_c(r,z) + P_b V_m(r,z))\left(1 + \alpha\left(\frac{r}{R}\right)^\beta\right) \quad (1)$$

where subscripts b and t denote the bottom and top surfaces of the plate and the subscripts c and m address the ceramic
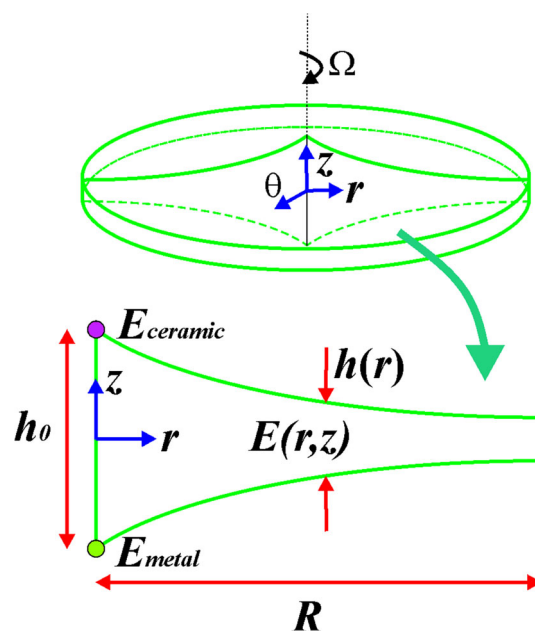

Fig. 1 The schematic view of the rotating micro-size tow-directional FGM variable thickness circular plate

and metal, respectively. α and β denote the coefficient and the power index of the material character variation in the radial-direction of the plate. In each material point of the microplate, it is obvious that:

$$V_c(r, z) + V_m(r, z) = 1 \tag{2}$$

Therefore, one rewrites Eq. (1) as follows:

$$P(r, z) = ((P_t - P_b)V_c(r, z) + P_b)\left(1 + \alpha\left(\frac{r}{b}\right)^{\beta}\right) \tag{3}$$

Assuming the origin of the coordinate in the center of the plate (as shown in Fig. 1), the volume fraction of the ceramic, V_c, would define in the power low form as follows:

$$V(r, z) = \left(\frac{1}{2} + \frac{z}{h}\right)^n \tag{4}$$

where n introduces the power index of the volume fraction.

Moreover, the variable thickness function, $h(r)$, is defined as follows:

$$h(r) = h_0\left(1 - q\left(\frac{r}{R}\right)^m\right) \tag{5}$$

in which q and m denote the coefficient and the power index for thickness-variation in radial-direction. Consequently, one would represent the Young's modulus expansion of the FGM material as follows:

$$E(r, z) = \left((E_c - E_m)\left(\frac{1}{2} + \frac{z}{h}\right)^n + E_m\right)\left(1 + \alpha\left(\frac{r}{R}\right)^{\beta}\right) \tag{6}$$

and for the simplicity of the formulation, it is summed that the mass density and the Poisson ratio variation as follows:

$$\rho(z) = \left((\rho_c - \rho_m)\left(\frac{1}{2} + \frac{z}{h}\right)^n + \rho_m\right) \tag{7}$$

$$v(z) = \left((v_c - v_m)\left(\frac{1}{2} + \frac{z}{h}\right)^n + v_m\right) \tag{8}$$

2.2 Governing equations of motion

In the three-dimensional first shear deformation plate theory, the displacement components (u_r, u_θ and u_z in cylindrical coordinate) of the circular plates would be written as follows:

$$u_r(r, \theta, z, t) = u(r, \theta, t) + z\Phi(r, \theta, t) \tag{9a}$$

$$u_\theta(r, \theta, z, t) = z\Psi(r, \theta, t) \tag{9b}$$

$$u_z(r, \theta, z, t) = w(r, \theta, z, t) \tag{9c}$$

where u and w are the radial and the transverse deflection, Φ and Ψ represent the rotations of a transverse normal line about r and θ coordinate, respectively. For the axisymmetric problem, the circumferential displacement, u_θ, is

omitted and Φ and w would be independent of the circumferential axis. Hence, displacement field would be rewritten as follows (Leissa 1969):

$$u_r(r, z, t) = u(r, t) + z\Phi(r, t) \tag{10a}$$

$$u_\theta(r, z, t) = 0 \tag{10b}$$

$$u_z(r, z, t) = w(r, z, t) \tag{10c}$$

thereafter, non-zero components of the linear strain tensor are written as follows (Leissa 1969):

$$\varepsilon_{rr}(r, z, t) = \frac{\partial u}{\partial r} + z\frac{\partial \Phi}{\partial r} \tag{11a}$$

$$\varepsilon_{\theta\theta}(r, z, t) = \frac{u}{r} + \frac{z}{r}\frac{\Phi}{r} \tag{11b}$$

$$\varepsilon_{rz}(r, z, t) = \frac{1}{2}\left(\frac{u}{r} + \frac{z}{r}\Phi\right) \tag{11c}$$

moreover, a non-zero component of the symmetric curvature tensor is (see "Appendix A"):

$$\chi_{r\theta} = \frac{1}{4}\left(\left(-\frac{\partial^2 w}{\partial r^2} + \frac{\partial \Phi}{\partial r}\right) - \left(\Phi - \frac{\partial w}{\partial r}\right)\right) \tag{12}$$

The strain energy of the circular microplate in axisymmetric condition would obtain by substituting the non-zero strain and the symmetric curvature strain components into Eq. (31) which lead to:

$$U = \frac{1}{2}\int_0^R \int_{-\frac{h(r)}{2}}^{\frac{h(r)}{2}}$$
$$\left[\begin{array}{l} \sigma_{rr}\left(\frac{\partial u}{\partial r} + z\frac{\partial \Phi}{\partial r}\right) + \sigma_{\theta\theta}\left(\frac{u}{r} + \frac{z}{r}\frac{\Phi}{r}\right) + 2\sigma_{rz}\left(\frac{1}{2}\left(\frac{u}{r} + \frac{z}{r}\Phi\right)\right) \\ +2m_{r\theta}\left(\frac{1}{4}\left(-\frac{\partial^2 w}{\partial r^2} + \frac{\partial \Phi}{\partial r}\right) - \frac{1}{4}\left(\Phi - \frac{\partial w}{\partial r}\right)\right) \end{array}\right] dz\,dr \tag{13}$$

Substituting the components of the stress tensor and the deviatoric part of the couple stress tensors (see "Appendix A") into Eq. (13), one could obtain the strain energy of the micro-plate as follows:

$$U = \frac{1}{2}\int_0^R$$
$$\left[\begin{array}{l} N_{rr}\frac{\partial u}{\partial r} + N_{\theta\theta}\frac{u}{r} + M_{rr}\frac{\partial \Phi}{\partial r} + N_{\theta\theta}\frac{\Phi}{r} + N_{rz}\left(\frac{\partial w}{\partial r} + \Phi\right) \\ +\frac{1}{2}\Omega_{r\theta}\left(\left(-\frac{\partial^2 w}{\partial r^2} + \frac{\partial \Phi}{\partial r}\right) - \frac{1}{r}\left(\Phi - \frac{\partial w}{\partial r}\right)\right) \end{array}\right] dr \tag{14}$$

where the forces, N_{ij}, the moments, M_{ij}, and the couple moment, Ω_{ij}, are defined in "Appendix B".

Since the kinetic energy of the plate, T, is extracted as follows:

$$T = \frac{1}{2} \int_0^R \int_{-\frac{h(r)}{2}}^{\frac{h(r)}{2}} \rho(r,z) \left[\left(\frac{\partial u}{\partial t} \right)^2 + \left(\frac{\partial v}{\partial t} \right)^2 + \left(\frac{\partial w}{\partial t} \right)^2 \right] dz dr \tag{15}$$

substituting the displacement components into Eq. (15) would lead to

$$T = \frac{1}{2} \int_0^R \int_{-\frac{h(r)}{2}}^{\frac{h(r)}{2}} \left[I_1 \left(\frac{\partial u}{\partial t} \right)^2 + 2I_2 \left(\frac{\partial u}{\partial t} \right) \left(\frac{\partial \Phi}{\partial t} \right) + I_3 \left(\frac{\partial \Phi}{\partial t} \right)^2 + I_1 \left(\frac{\partial w}{\partial t} \right)^2 \right] dz dr \tag{16}$$

where the constants are defined as follows:

$$\{I_1, I_2, I_3\} = \int_{-\frac{h(r)}{2}}^{\frac{h(r)}{2}} \rho(r,z)\{1, z^1, z^2\} dz \tag{17}$$

and the external work, H (due to the rotation) could present as (Bauer and Eidel 2007):

$$H = \frac{1}{2} \int N^{Rotation} \left(\frac{\partial w}{\partial r} \right)^2 dA \tag{18}$$

where N^{Rotation} represents the radial-direction force due to the circumferential acceleration of the angular velocity, Ω, which is defined as follows (Bauer and Eidel 2007):

$$N^{rotation} = \int_{-\frac{h(r)}{2}}^{\frac{h(r)}{2}} \left(\frac{\rho \, \Omega^2}{8} (2(r)(3+v)) \right) dz \tag{19}$$

The governing equations of motion for a rotating variable thickness two-directional FG circular microplate would be extracted utilizing Hamilton's principle as follows:

$$\delta \int_0^t (-U + T + H) = 0 \tag{20}$$

where δ is the variation operator.

Substituting Eqs. (14), (16), and (18) into Eq. (20), the governing equations of motion and the associated boundary conditions would be obtained:

$$\frac{1}{r} \frac{\partial}{\partial r} (rN_r) - (N_\theta) = I_1 \frac{\partial^2 u}{\partial t^2} + I_2 \frac{\partial^2 \Phi}{\partial t^2} \tag{21a}$$

$$\frac{1}{2r} \frac{\partial^2}{\partial r^2} (r\Omega_{r\theta}) + \frac{1}{2r} \frac{\partial}{\partial r} (\Omega_{r\theta}) + \frac{1}{2r} \frac{\partial}{\partial r} (rN_{rz}) \\ + \frac{\partial}{r\partial r} \left(N^{Rotation} r \frac{\partial w}{\partial r} \right) + F \\ = I_1 \frac{\partial^2 w}{\partial t^2} \tag{21b}$$

$$\frac{1}{2r} \frac{\partial^2}{\partial r^2} (r\Omega_{r\theta}) + \frac{\Omega_{r\theta}}{2r} + \frac{1}{r} \frac{\partial}{\partial r} (rM_r) - \frac{M_\theta}{r} - N_{rz} \\ = I_2 \frac{\partial^2 u}{\partial t^2} + I_3 \frac{\partial^2 \Phi}{\partial t^2} \tag{21c}$$

$$(N_r)\delta u = 0 \quad \text{at r = 0, R} \tag{21d}$$

$$\left(\frac{1}{2r} \frac{\partial}{\partial r} (r\Omega_{r\theta}) + \frac{\Omega_{r\theta}}{2r} + N_{rz} - N_r \frac{\partial w}{\partial r} \right) \delta w = 0 \quad \text{at r = 0, R} \tag{21e}$$

$$\frac{r\Omega_{r\theta}}{2r} \frac{\partial}{\partial r} (\delta w) = 0 \quad \text{at r = 0, R} \tag{21f}$$

$$\left(M_{rr} + \frac{\Omega_{r\theta}}{2} \right) (\delta \Phi) = 0 \quad \text{at r = 0, R} \tag{21g}$$

The governing equations of motion and the associated boundary conditions in terms of displacement components are presented in "Appendix C".

2.3 Solution method

In order to solve the governing equations of motion with the associated boundary conditions (see "Appendix C") for free vibration of a rotating variable thickness two-directional FG circular microplate, DQ method is utilized. In this method, weight coefficients are computed by an algebraic equation system which confined the usage of large grid numbers. The discretization rule of the method enables one to approximate m-th derivatives of displacement functions, u, w and Φ in respect to r that are defined as the linear sum of the function values (Shu 2012):

$$\frac{\partial^m \{u(r), w(r), \Phi(r)\}}{\partial r^m} \bigg|_{r=r_p} = \sum_{k=1}^n C_{ik}^{(m)} \{u_k, w_k, \Phi_k\} \tag{22}$$

where

$$u_k = u(r_k, t) \tag{23a}$$

$$w_k = w(r_k, t) \tag{23b}$$

$$\Phi_k = \Phi(r_k, t) \tag{23c}$$

n represents the total number of grid points distributed along the r-axis and $C_{ik}^{(m)}$ is the weighting coefficients whose recursive formula can be found in as follows:

$$C_{ik}^{(1)} = \begin{cases} \dfrac{M(r_i)}{(r_i - r_k)M(r_k)} & i \neq k \\ -\sum\limits_{k=1, i \neq k}^{n} C_{ik}^{(1)} & i = k \end{cases} \qquad (24)$$

where k = 1,2,3, …, n. The more accurate the weight coefficient with an appropriate selection of the grid points, the more accurate the solution of the equations.

In order to improve the mesh point distribution, the cosine pattern, as known Chebyshev–Gauss–Lobatto technique, is used to generate the DQ points as follows:

$$r_i = \frac{1}{2}\left(1 - \cos\left(\frac{(i-1)}{(n-1)}\pi\right)\right) \qquad (25)$$

where i = 1,2,3, …, n. The analysis indicates that the above distribution would accelerate the convergence of the solution. $M(r)$ is defined as follows:

$$M(r) = \prod_{k=1, k \neq i}^{n} (r_i - r_k) \qquad (26)$$

The associated weighting coefficient for r-th derivative of displacement functions is written as follows:

$$C_{ik}^{(m)} = \begin{cases} m\left[C_{ik}^{(m-1)}C_{ik}^{(1)} - \dfrac{C_{ik}^{(m-1)}}{(r_i - r_k)}\right] & i \neq k \ and \ 2 \leq m \leq n-1 \\ -\sum\limits_{k=1, i \neq k}^{n} C_{ik}^{(m)} & i = k \ and \ 1 \leq m \leq n-1 \end{cases} \qquad (27)$$

Applying DQ method into the governing equations of the rotating variable thickness two-directional FG circular microplate in terms of displacement components (see "Appendix C") would lead to the discretized governing equations of motion which are presented in "Appendix D".

Now, one would rewrite the governing equations of motion in matrix form as follows:

$$M\frac{\partial^2 d}{\partial t^2} + K_e d = 0 \qquad (28)$$

where M and K_e, are the mass matrix and stiffness matrix, respectively. Utilizing the first shear deformation theory, the dimensions of matrices would be $3N \times 3N$ where the unknown displacement vector, d, is defined as follows:

$$d = \{\{u_i\}^T, \{w_i\}^T, \{\Phi_i\}^T\} \qquad (29)$$

Equation (28) would be utilized for the free vibration analysis of the rotating variable thickness two-directional FG circular microplate. Moreover, the critical angular velocity of the structure which referred to the unstable condition of the microplate could be obtained in the parametric studies.

3 Results and discussion

In this section, the first natural frequencies results for a rotating variable thickness two-directional FG circular microplate are presented. The non-dimensional angular velocity, Ω^*, of the microplate, is defined as follows:

$$\Omega^* = \frac{\Omega}{\sqrt{D_{11}^c/(I_1^c \times R^4)}} \qquad (30)$$

where, the superscript c is addressed as a ceramic material. The results obtained in this study are verified with the available results in the literature and then the effects of the angular velocity, the thickness variation, the two-directionality of FG material, the size dependency, and the boundary condition on the first non-dimensional natural frequencies are studied.

3.1 Verification

Leissa (1969) presented an analytical solution for the free vibration of a circular classical plate. Moreover Yalcin et al. (2009) and Wu et al. (2002) determined the natural frequencies of the circular classical plates utilizing differential transformation method (DTM) and generalized differential quadrature (GDQ), respectively. In order to compare the results, a reduced form of the proposed formulation would be obtained by assuming that $\Phi = -\partial w/\partial r$ in Eqs. (10a–10c).

In Table 1, the first five non-dimensional natural frequencies for a circular classical plate obtained in this study are compared with those available results in the literature (Leissa 1969; Yalcin et al. 2009; Wu et al. 2002) The results are presented for different boundary conditions, hinged and clamped. As can be seen, there is a very good agreement between results, indicating the accuracy of the formulation and the solution procedure for the classical plate, neglecting the size dependency effects.

Moreover, in Table 2, the free vibration results obtained in this study are compared with those available results in the literature (Liew et al. 1997; Irie et al. 1980) for a circular plate utilizing first shear deformation theory, indicating a very good agreement.

In order to evaluate the proposed formulation for a two-dimensional FG material circular plate, a comparison between obtained results in this study and those available results in the literature (Shariyat and Alipour 2013) is conducted in Table 3. The analyses reveal an acceptable agreement between results.

Table 1 The comparison of the first five non-dimensional natural frequencies results, ω, for a circular plate obtained in this study with those presented in the (Leissa 1969; Yalcin et al. 2009; Wu et al. 2002) utilizing the classical theory (R/h = 20)

B.C.	Mode	Present study (DQM)	(Leissa 1969) (exact)	(Yalcin et al. 2009) (DTM)	(Wu et al. 2002) (GDQ)
Hinged	1	4.9351	4.997	4.9351	4.935
	2	29.7199	29.76	29.72	29.72
	3	74.1559	74.2	74.1561	74.156
	4	138.3179	138.34	138.3181	138.318
	5	222.2145	–	222.215	222.215
Clamped	1	10.2158	10.2158	10.2158	10.216
	2	39.7711	39.771	39.7711	39.771
	3	89.1040	89.104	89.1041	89.104
	4	158.1839	158.183	158.1842	158.184
	5	247.0059	247.005	247.0064	247.006

Table 2 The comparison of the first five non-dimensional natural frequencies, ω, of a circular plate obtained in this study with those presented in the literature (Liew et al. 1997; Irie et al. 1980) utilizing the first shear deformation theory

B.C.	Mode	Present study (DQM)	(Liew et al. 1997) (DQ) _ENREF_14	(Irie et al. 1980) (Exact)	Present study (DQM)	(Liew et al. 1997) (DQ)	(Irie et al. 1980) (Exact)
		R/h = 1000			R/h = 4		
Hinged	1	4.9353	4.9351	4.935	4.6963	4.6963	4.696
	2	29.720	29.720	29.720	23.254	23.254	23.254
	3	74.155	74.155	74.156	46.774	46.775	46.775
	4	138.31	138.31	138.318	71.602	71.603	71.603
	5	222.21	222.21	–	96.608	96.609	–
Clamped	1	10.216	10.216	10.216	8.8068	8.8068	8.807
	2	39.771	39.771	39.771	27.253	27.253	27.253
	3	89.102	89.102	89.102	49.420	49.420	49.420
	4	158.18	158.18	158.184	73.054	73.054	73.054
	5	246.99	246.99	–	97.198	97.198	–

3.2 Parametric study

In order to perform a parametric study on the free vibration behavior of a variable thickness two-directional FG circular microplate, the verified proposed formulation would be utilized. The effects of the thickness-variation, the two-directionality-variation of the material and the size dependency on the non-dimensional natural frequencies of a circular microplate in terms of the non-dimensional angular velocity are studied.

3.2.1 Thickness-variation effect

In order to evaluate the thickness-variation effects on the non-dimensional natural frequency of a rotating two-directional FG circular microplate, in Table 4, the results for different boundary conditions as well as angular velocities are presented. It can be seen the fact that increasing the angular velocity would lead the reduction in the non-dimensional natural frequencies and, moreover, the non-dimensional natural frequencies of the clamped plates are larger than those of the hinged ones. The both are because of the effective stiffness variation in the plates. As considered in Table 4, the variation of the non-dimensional natural frequencies in terms of the thickness-variation index, m, is not proportional. In the case $m = 0$, there is a uniform thickness plate (the thickness is equal to h_0) with a two-directional FG material. Increasing m from 0 to 1, the uniform thickness plate is converting to a plate with a central thickness equal to h_0 and a linear thickness reduction to $h_0/2$ at the outer radius. In this case, due to a large reduction in effective stiffness of the plate in comparison with the mass reduction of that, the non-dimensional natural frequency is decreased with respect to those observed

Table 3 The comparison of the first third non-dimensional natural frequencies of two-directional FGM circular plates obtained in this study with those presented in the literature

B.C.	Mode	Present study (DQM), n = 0.2	(Shariyat and Alipour 2013) (DTM), n = 0.2	Present study (DQM), n = 2	(Shariyat and Alipour 2013) (DTM), n = 2	Present study (DQM), n = 0.2	(Shariyat and Alipour 2013) (DTM), n = 0.2	Present study (DQM), n = 2	(Shariyat and Alipour 2013) (DTM), n = 2
		$\beta = 2, \alpha = 0.5$				$\beta = 4, \alpha = 0.5$			
Hinged	1	4.92078	4.959189	3.71492	3.9298	4.76340	4.79814	3.64116	3.80222
	2	29.7261	29.96814	22.2568	23.74785	28.6907	28.9284	21.4185	22.9239
	3	74.0722	74.67712	55.4163	59.17691	71.7757	72.3747	53.6166	57.3524
		$\beta = 2, \alpha = -0.5$				$\beta = 4, \alpha = -0.5$			
	1	4.18313	4.218785	3.11254	3.343120	4.37398	4.41483	3.19545	3.49847
	2	24.9063	25.10470	18.7440	19.89388	26.2034	26.4073	19.8241	20.9261
	3	62.1123	62.61459	46.5817	49.61810	65.0230	65.4732	48.9484	51.8834
		$\beta = 2, \alpha = 0.5$				$\beta = 4, \alpha = 0.5$			
Clamped	1	10.5847	10.66458	8.03596	8.451005	10.31334	10.3881	7.88106	8.23195
	2	40.1541	40.47366	30.1881	32.07281	39.05298	39.3632	29.3720	31.1928
	3	89.3860	90.10920	67.0049	71.40582	86.93443	87.6448	65.1909	69.4530
		$\beta = 2, \alpha = -0.5$				$\beta = 4, \alpha = -0.5$			
	1	8.0428	8.116881	5.87263	6.432114	8.354452	8.43586	6.01613	6.68488
	2	32.6569	32.93335	24.2786	26.09760	33.98871	34.2785	25.2368	27.1635
	3	73.9200	74.53463	55.1244	59.06397	76.92765	77.5327	57.3480	61.4398

Table 4 The comparison of results obtained by first shear deformation theory for the first non-dimensional natural frequency of a rotating two-directional FG circular microplate for different non-dimensional angular velocities, boundary conditions and thickness variations ($h/l = 1$, $\alpha = 0.5$, $\beta = 2$, $n = 2$, $R/h = 20$, $q = 0.5$)

B.C.	M	$\Omega^* = 0$	$\Omega^* = 10$	$\Omega^* = 30$
Hinged	0	68.7938347255210	68.6040017111398	66.5793716006974
	1	38.3926911553748	37.2021895427589	29.1354031568160
	2	63.7490610343833	63.4570694044919	60.5937766539455
	3	64.7710411293419	64.4555756606505	61.3597102113318
	4	65.0988788079747	64.7771189145610	61.6102662528111
	5	69.0396734230879	68.6609222158449	65.0197607098747
Clamped	0	70.4605478633893	70.3255824627969	68.8380345407913
	1	45.5530269827272	44.2880393912905	35.4084604393587
	2	65.6046212463317	65.3865666984312	63.2315853749363
	3	66.9488415844630	66.7079413565841	64.3503808093305
	4	67.5304472799265	67.2861864931913	64.8887743114389
	5	72.1315237224300	71.8377543075618	69.0566743707141

for the first uniform thickness plate. However, it depends on where the thickness is decreased in the section of the plate, the non-dimensional natural frequency might increase or decrease. The fact is that due to two-directionality-variations in the material property (as known non-homogeneous material), there is no a proportional relation between the non-dimensional natural frequency and the thickness variation, unlike the proportional relation could be observed in a homogeneous material plate.

In Figs. 2 and 3, the first two non-dimensional natural frequencies of a rotating two-directional FG circular microplate in terms of the non-dimensional angular velocity for different variations of thickness prescribed by clamp and hinge boundary conditions are presented, respectively. Although, the non-dimensional natural frequencies of the plates vary with respect to the thickness variation, the results reveal that the critical angular velocity would be insensitive in respect to that.

In Figs. 4 and 5, the first non-dimensional natural frequencies for a two-directional FG circular microplate in terms of the non-dimensional natural frequency for different rates, q, of the linear thickness variation, $m = 1$, with the clamped and the hinged boundary condition are presented, respectively. As can be seen, the more rate of
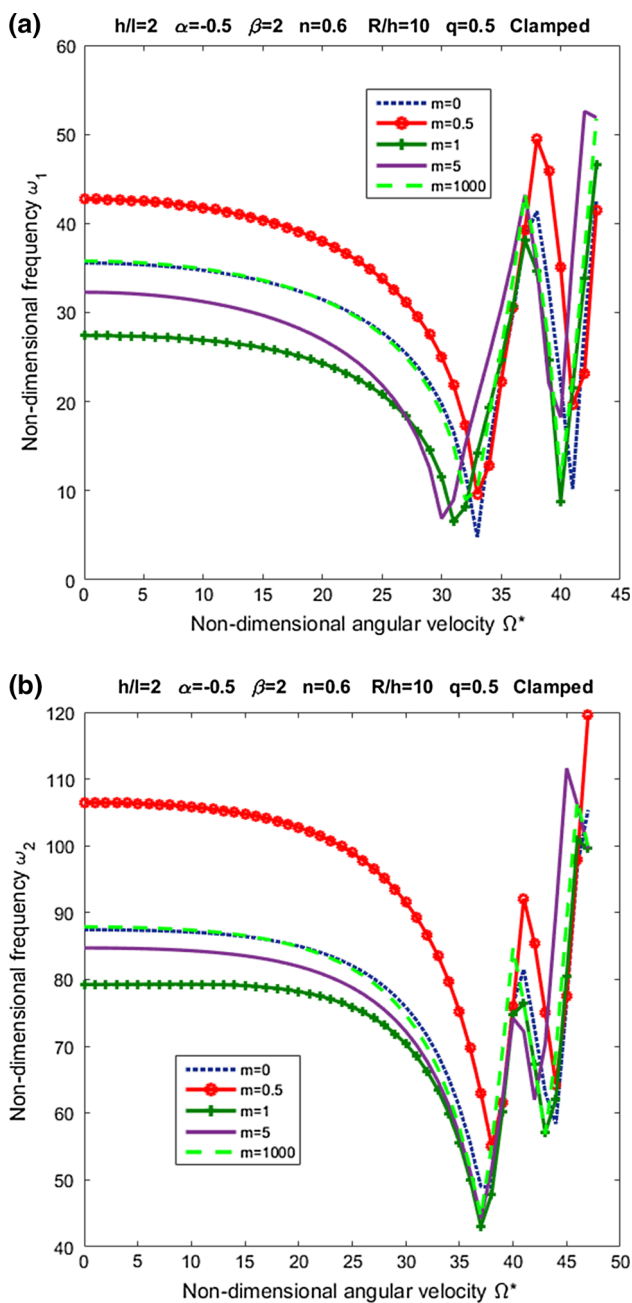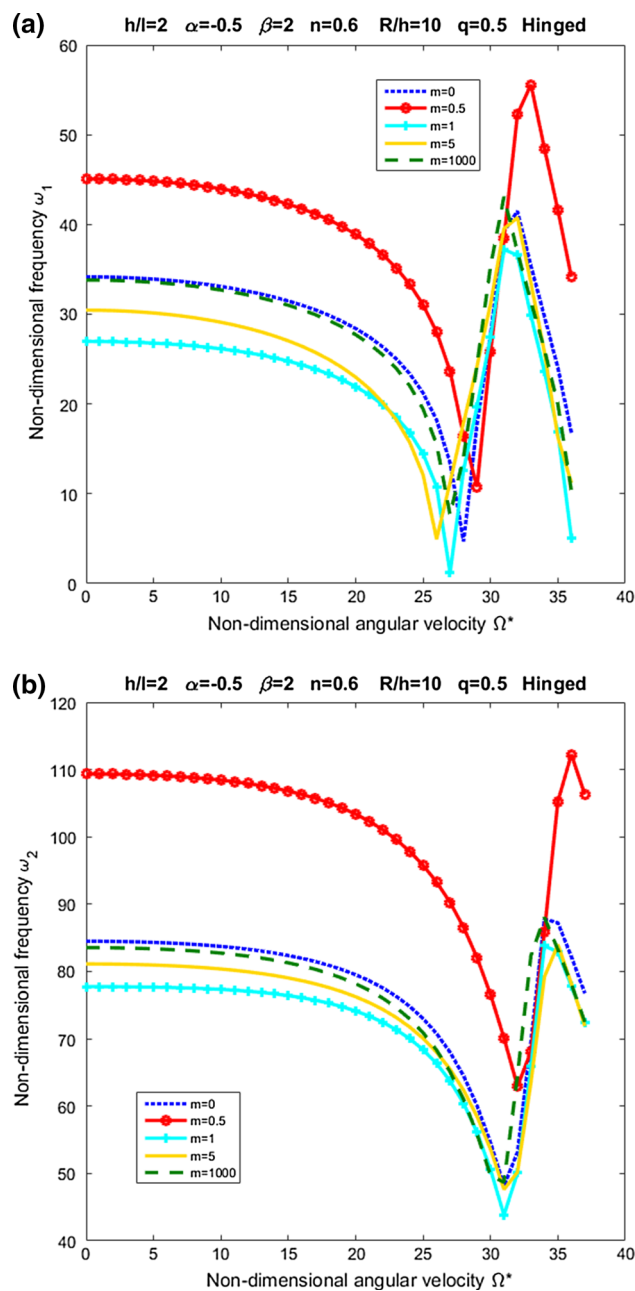
(a)

(b)

Fig. 2 Free vibration of rotating two-directional FGM circular microplates in terms of the non-dimensional angular velocity for different variations of the thickness with the clamped boundary condition: **a** the first non-dimensional natural frequencies, ω_1, **b** the second non-dimensional natural frequencies, ω_2

(a)

(b)

Fig. 3 Free vibration of rotating two-directional FGM circular microplates in terms of the non-dimensional angular velocity for different variations of thickness with the hinged boundary condition: **a** the first non-dimensional natural frequencies, ω_1, **b** the second non-dimensional natural frequencies, ω_2

the linearly increasing the thickness in the microplate, the more enlargement of the effective stiffness. Since the linearly varying the thickness has a significant proportional effect on the critical angular velocity of the clamped microplate, this could be neglect about the hinged ones, as can be seen in Figs. 4 and 5.

3.2.2 Two-directionality-variation in FG material effect

In order to study the impact of two-directionality-variation of FG material, in Table 5, the first non-dimensional natural frequencies of a rotating variable thickness circular microplate for different size dependencies, h/l, and the material coefficients in radial-direction, α, are presented. The results are evaluated for the hinged and the clamped
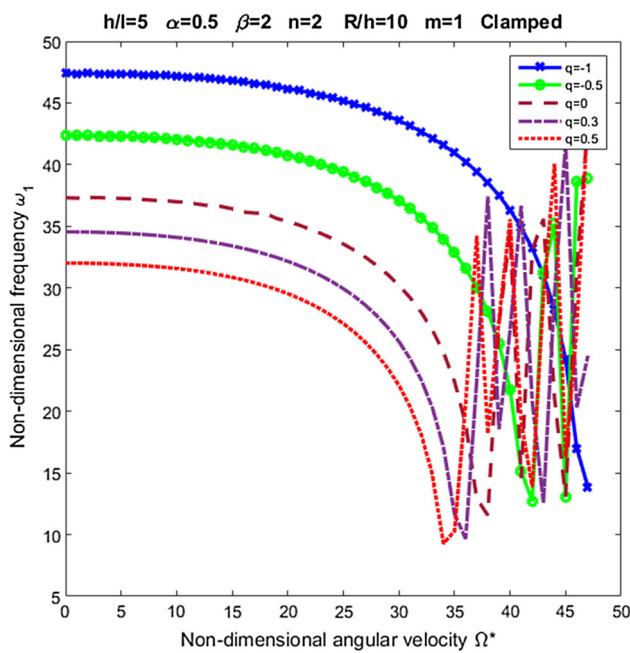
Fig. 4 The first non-dimensional natural frequency, ω_1, of a clamped two-directional FG circular microplate in terms of non-dimensional angular velocity for different rates of the linear thickness variation
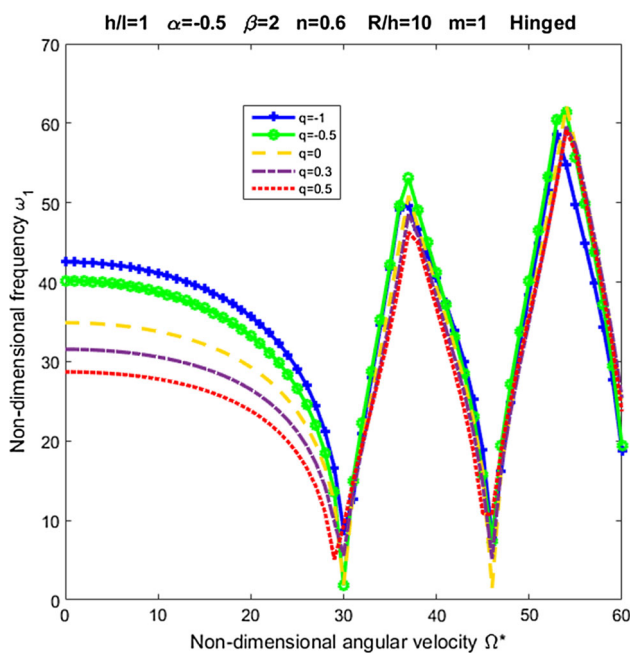

Fig. 5 The first non-dimensional natural frequency, ω_1, of a hinged two-directional FG circular microplate in terms of non-dimensional angular velocity for different rates of the linear thickness variation

microplates. As discussed in the literature, there is a critical size dependency in which a significant reduction would occur in the first non-dimensional natural frequencies of the structure. This was known as buckling phenomenon in the literature. For instance, in the case of hinged one-dimensional FG microplate, (i.e. $\alpha = 0$), in Table 5, h/l close

to 1 could know as a critical value. Considering the variation of material in the two-direction, (i.e. $\alpha = -0.5$ and 0.5), would lead to the increase or the decrease in the critical values, as can be seen in Table 5. Moreover, it is clear that the non-dimensional natural frequencies of the microplate strongly are depending on how the material is graded in the plate. This could be found that the effects of the material variation in the second direction would lead to non-proportionality of the mechanical response of the plate. Therefore, the nonlinear effects of the material variation on the response of such plates should be predicted to the design of the microdevices.

Moreover, in Fig. 6, the variation of the first and the second non-dimensional natural frequencies of a rotating variable thickness circular microplate in terms of the non-dimensional angular velocity for one- and two-direction FG materials are presented. Not only the material variation in the second direction has a significant effect on the non-dimensional natural frequencies, but also there is an ineligible impact on the critical angular velocities, as can be found in Fig. 6.

In Fig. 7, the first three non-dimensional natural frequencies of rotating variable thickness circular microplate in terms of the FG power index in the thickness direction, n, for homogeneous, one- and two-direction FG materials are presented. The homogeneous material plate is associated with the case of $n = \alpha = 0$. It can be seen, replacing the homogeneous material with one-directional FG material, $\alpha = 0$, and $n \neq 0$ would lead a reduction in the first non-dimensional natural frequencies. This is because of the effective stiffness reduction in the FG plate in comparison with the first one. Moreover, it can be found in Fig. 7, the effects of two-directionality-variation of FG material, α, is not sensitive in respect to FG power index in the thickness direction, n.

The impact of FG power index in the thickness direction, n, on the first non-dimensional natural non-dimensional frequency in terms of the non-dimensional angular velocity, could be seen in Figs. 8 and 9 for a variable thickness circular microplate prescribed by clamp and hinge boundary conditions, respectively. In the cases of $n = 0$ and 1000 (infinity), there is only the radially graded material (one-directional FG) with the homogeneous ceramic and metal in thickness direction, respectively. As can be found in Figs. 8 and 9, there is a proportional relation between the FG power index in the thickness direction, n, and the first non-dimensional natural frequency as well as the critical angular velocity.

Moreover, the proportional effects of the FG power index in the radial direction, β, on the first non-dimensional natural frequency in terms of the non-dimensional angular velocity could be seen in Fig. 10, where the cases of $\beta = 0$ and 1000 (infinity), are known as thickness-dependent graded materials.

Table 5 The size dependency effects on the first non-dimensional natural frequency, ω_1, of a rotating variable thickness circular microplate subjected to different boundary conditions and two-direction FG materials ($m = 1$, $\Omega^* = 0.5$, $\beta = 2$, $n = 1.2$, $R/h = 15$, $q = 0.5$)

B.C.	H/l	$\alpha = -0.5$	$\alpha = 0$	$\alpha = 0.5$
Hinged	0	35.5342464161960	39.4342059602109	8.93905142001673
	1	22.3929925454333	26.2201843156676	87.8393475216015
	2	50.8670861477480	66.6968776342821	85.0169157181622
	3	41.5471243701925	55.5693909935267	72.5933640232347
	4	39.3145792009598	51.9813307948652	66.2871075115930
	5	38.2966557460600	50.2418785521676	62.6821309017845
	6	37.7154673782919	49.2281213084505	60.4118029378133
	7	37.3378214880814	48.5692985263160	58.8749818646699
	8	37.0777574854644	48.1205591832066	43.4901012072814
	9	36.8881282401072	47.7941670355355	56.9947071141607
	10	35.5342464161960	39.4342059602109	8.93905142001673
Clamped	0	32.1699435014637	36.7204657974089	6.41516837292463
	1	28.2043846777705	24.1731372625965	54.1456054753421
	2	22.8377392650436	19.4336771284445	77.9839711542219
	3	15.0110177292492	37.5138173132953	92.9455164114897
	4	6.00980233158180	44.7738103746764	97.4416206394684
	5	8.04693951659633	43.0114950090936	92.3156372331641
	6	15.9258079807402	34.4212762986930	81.1073315876968
	7	21.7680621774675	20.9209761966145	67.5353197667057
	8	25.6298610445980	13.0178705282108	80.2905921057517
	9	28.1487596479929	24.6551909055820	41.1818763118726
	10	32.1699435014637	36.7204657974089	6.41516837292463

In Fig. 11, a comprehensive map for the two-directionality-variation of material effects on the first three non-dimensional natural frequencies of a rotating variable thickness circular microplate is presented. The area between the upper and the lower curves is associated with the non-dimensional natural frequencies for a two-direction FG plate and the boundaries of the area are associated with those for one-direction FG plates.

3.2.3 Size dependency effect

In Figs. 12 and 13, the impact of the size dependency on the first non-dimensional natural frequency for a variable thickness circular microplate in terms of the non-dimensional angular velocity with clamped and hinged boundary conditions are presented, respectively. As can be seen, the increase of the size dependency would lead to the reduction of the non-dimensional natural frequency as well as critical angular velocity.

4 Conclusion

In this paper, the governing equations of motion for a rotating variable thickness two-directional FG circular microplate were proposed. The equations were derived utilizing the Hamiltonian's principle as well as the first shear deformation and the modified couple stress theories. The differential quadrature method was used to pursue the solution procedure. The proposed formulation, in special cases, was verified with the available results in the literature. The contributions of the thickness-variation of the section, two-directionality-variation of the material and the size dependency as well as the angular velocity of the plate, on the first natural frequencies were studied.

Appendix A

The strain energy, U, in an isotropic linear elastic material would obtain utilizing the modified couple stress theory as follows (Eshraghi et al. 2016; Reddy and Berry 2012; Ke et al. 2012):

$$U = \frac{1}{2} \int_V (\sigma : \varepsilon + m : \chi) dV \tag{31}$$

where ε and σ are the linear strain and the Cauchy stress tensors, respectively. χ and m are the symmetric curvature strain and deviatoric part of the couple stress tensors. The four last tensors are defined as follows (Eshraghi et al. 2016; Reddy and Berry 2012; Ke et al. 2012):
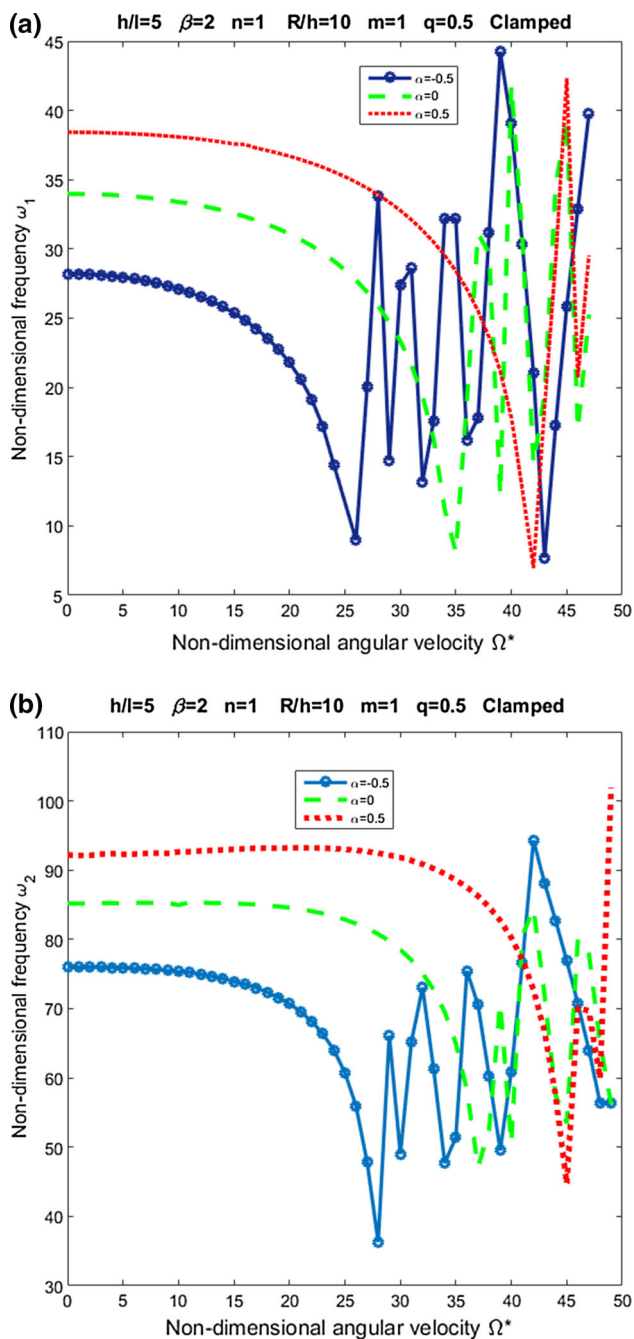
(a) h/l=5 β=2 n=1 R/h=10 m=1 q=0.5 Clamped

(b) h/l=5 β=2 n=1 R/h=10 m=1 q=0.5 Clamped

Fig. 6 Free vibration of a rotating variable thickness circular microplate in terms of the non-dimensional angular velocity for one- and two-direction FG materials: **a** the first non-dimensional natural frequencies, ω_1, **b** the second non-dimensional natural frequencies, ω_2

$$\sigma = \lambda tr(\varepsilon)I + 2\mu\varepsilon \tag{32}$$

$$\varepsilon = \frac{1}{2}[\nabla u + (\nabla u)^T] \tag{33}$$

$$m = 2l^2\mu\chi \tag{34}$$

$$\chi = \frac{1}{2}[\nabla \Lambda + (\nabla \Lambda)^T] \tag{35}$$

where λ and μ are the Lame's constant, u and l are the displacement vector and the material length scale parameter, respectively, and Λ is a rotation vector defined by:

$$\Lambda = \frac{1}{2}curl u \tag{36}$$

Appendix B

$$N_{rr}(r) = \int_{-\frac{h(r)}{2}}^{\frac{h(r)}{2}} \sigma_{rr}dz = \left(A_{11}(r)\frac{\partial u}{\partial r} + A_{12}(r)\frac{u}{r}\right)$$
$$+ \left(B_{11}(r)\frac{\partial \Phi}{\partial r} + B_{12}(r)\frac{\Phi}{r}\right) \tag{37}$$

$$N_{\theta\theta}(r) = \int_{-\frac{h(r)}{2}}^{\frac{h(r)}{2}} \sigma_{\theta\theta}dz = \left(A_{12}(r)\frac{\partial u}{\partial r} + A_{11}(r)\frac{u}{r}\right)$$
$$+ \left(B_{12}(r)\frac{\partial \Phi}{\partial r} + B_{11}(r)\frac{\Phi}{r}\right) \tag{38}$$

$$M_{rr}(r) = \int_{-\frac{h(r)}{2}}^{\frac{h(r)}{2}} \sigma_{rr}z dz = \left(B_{11}(r)\frac{\partial u}{\partial r} + B_{12}(r)\frac{u}{r}\right)$$
$$+ \left(A_{11}(r)\frac{\partial \Phi}{\partial r} + B_{12}(r)\frac{\Phi}{r}\right) \tag{39}$$

$$M_{\theta\theta}(r) = \int_{-\frac{h(r)}{2}}^{\frac{h(r)}{2}} \sigma_{\theta\theta}z dz = \left(B_{12}(r)\frac{\partial u}{\partial r} + B_{11}(r)\frac{u}{r}\right)$$
$$+ \left(D_{11}(r)\frac{\partial \Phi}{\partial r} + D_{12}(r)\frac{\Phi}{r}\right) \tag{40}$$

$$M_{rz}(r) = \int_{-\frac{h(r)}{2}}^{\frac{h(r)}{2}} \sigma_{rz}dz = k_s A_{55}(r)\left(\frac{\partial w}{\partial r} + \Phi\right) \tag{41}$$

$$\Omega_{r\theta} = \int_{-\frac{h(r)}{2}}^{\frac{h(r)}{2}} m_{r\theta}dz = \frac{1}{2}S(r,z)\left(\left(\frac{\partial \Phi}{\partial r} - \frac{\partial^2 w}{\partial r^2}\right) - \frac{1}{r}\left(\Phi - \frac{\partial w}{\partial r}\right)\right) \tag{42}$$

where ks = $\pi^2/12$ is known as the shear correction factor and the constants are defined as follows:
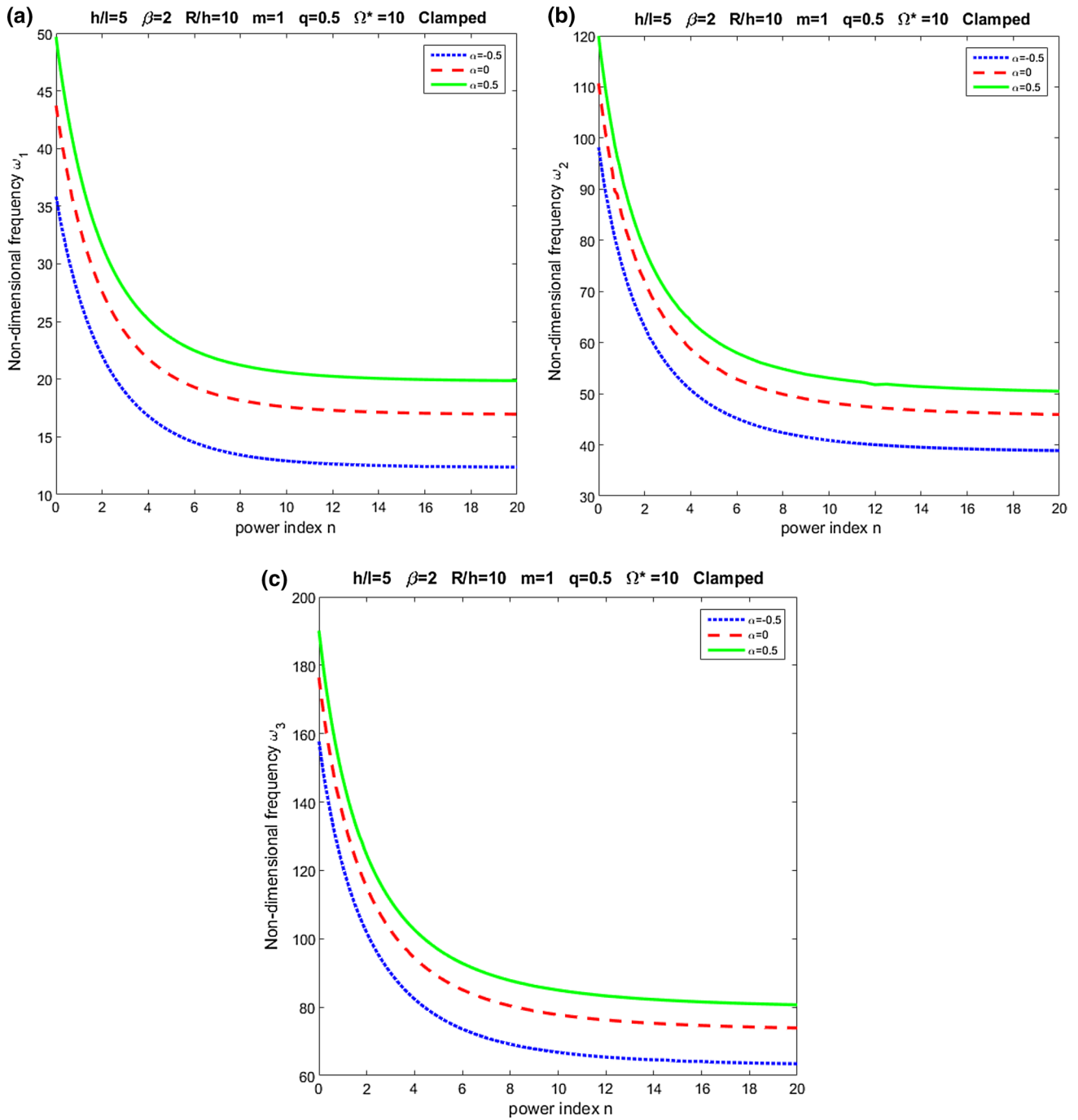
Fig. 7 free vibration of a rotating variable thickness circular microplate in terms of the FG power index for homogeneous, one- and two-direction FG materials: **a** the first non-dimensional natural frequencies, ω_1, **b** the second non-dimensional natural frequencies, ω_2, **c** the third non-dimensional natural frequencies, ω_3
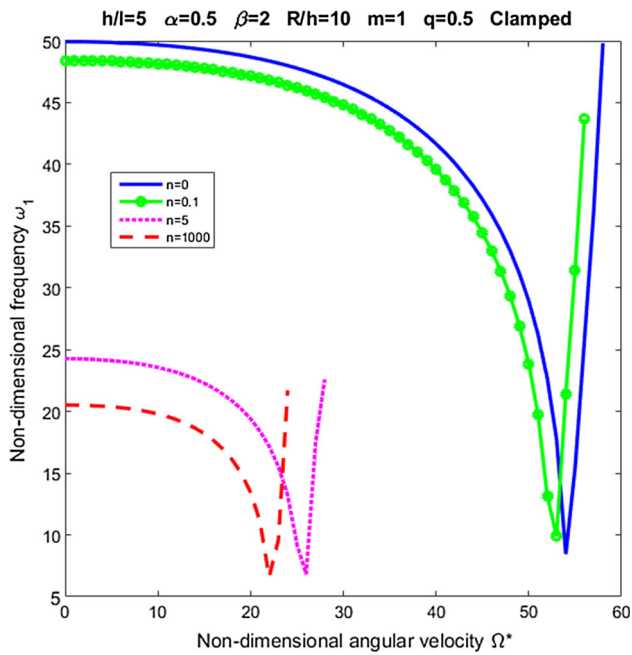
Fig. 8 The first non-dimensional natural frequency of a clamped variable thickness circular microplate in terms of the non-dimensional angular velocity for one- and two-direction FG materials (the impact of FG power index in thickness direction, n)
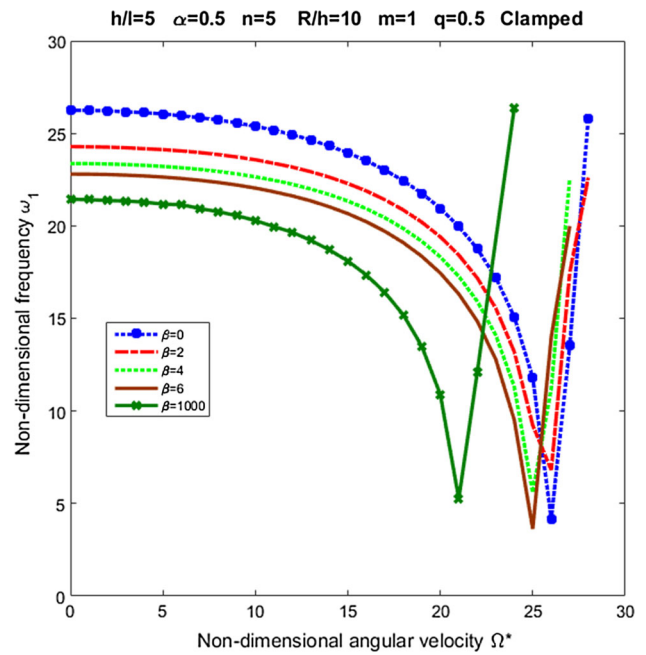
Fig. 10 The first natural non-dimensional frequency of a clamped variable thickness circular microplate in terms of the non-dimensional angular velocity for one- and two-direction FG materials (the impact of FG power index in radial direction, β)

$$\{A_{11}, B_{11}, D_{11}\} = \int_{-\frac{h(r)}{2}}^{\frac{h(r)}{2}} \left(\frac{E(r,z)}{1 - v^2(r,z)}\right) \{1, z, z^2\} dz \tag{43}$$

$$\{A_{12}, B_{12}, D_{12}\} = \int_{-\frac{h(r)}{2}}^{\frac{h(r)}{2}} \left(\frac{E(r,z)v(z)}{1 - v^2(r,z)}\right) \{1, z, z^2\} dz \tag{44}$$

$$A_{55} = \int_{-\frac{h(r)}{2}}^{\frac{h(r)}{2}} \left(\frac{E(r,z)}{2(1 + v(r,z))}\right) dz \tag{45}$$

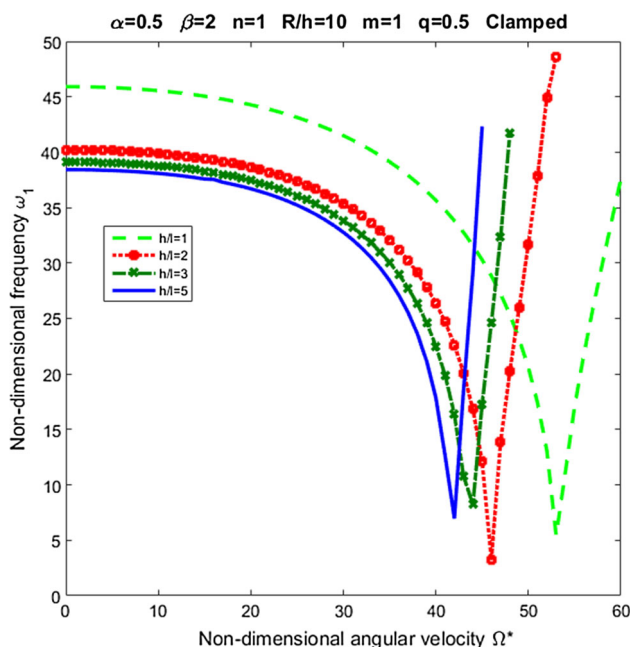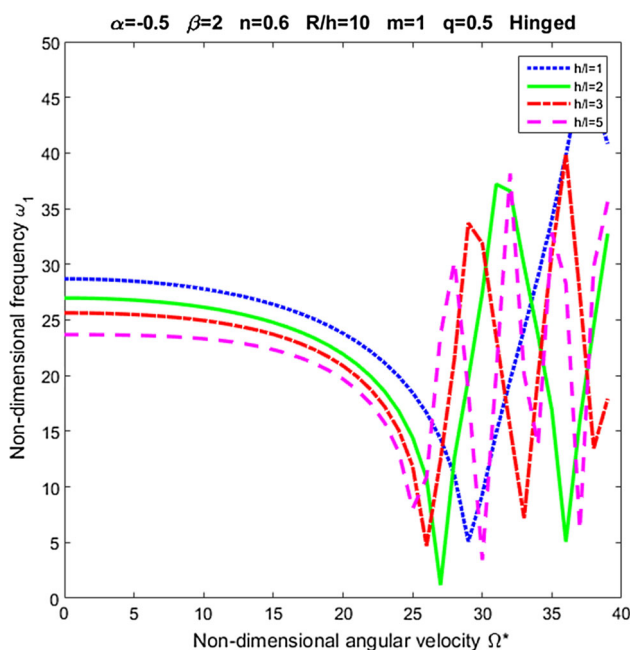$$S = \int_{-\frac{h(r)}{2}}^{\frac{h(r)}{2}} \left(\frac{l^2(r,z)E(r,z)}{2(1 + v(r,z))}\right) dz \tag{46}$$

Fig. 9 The first non-dimensional natural frequency of a clamped variable thickness circular microplate in terms of the non-dimensional angular velocity for one- and two-direction FG materials (the impact of FG power index in thickness direction, n)
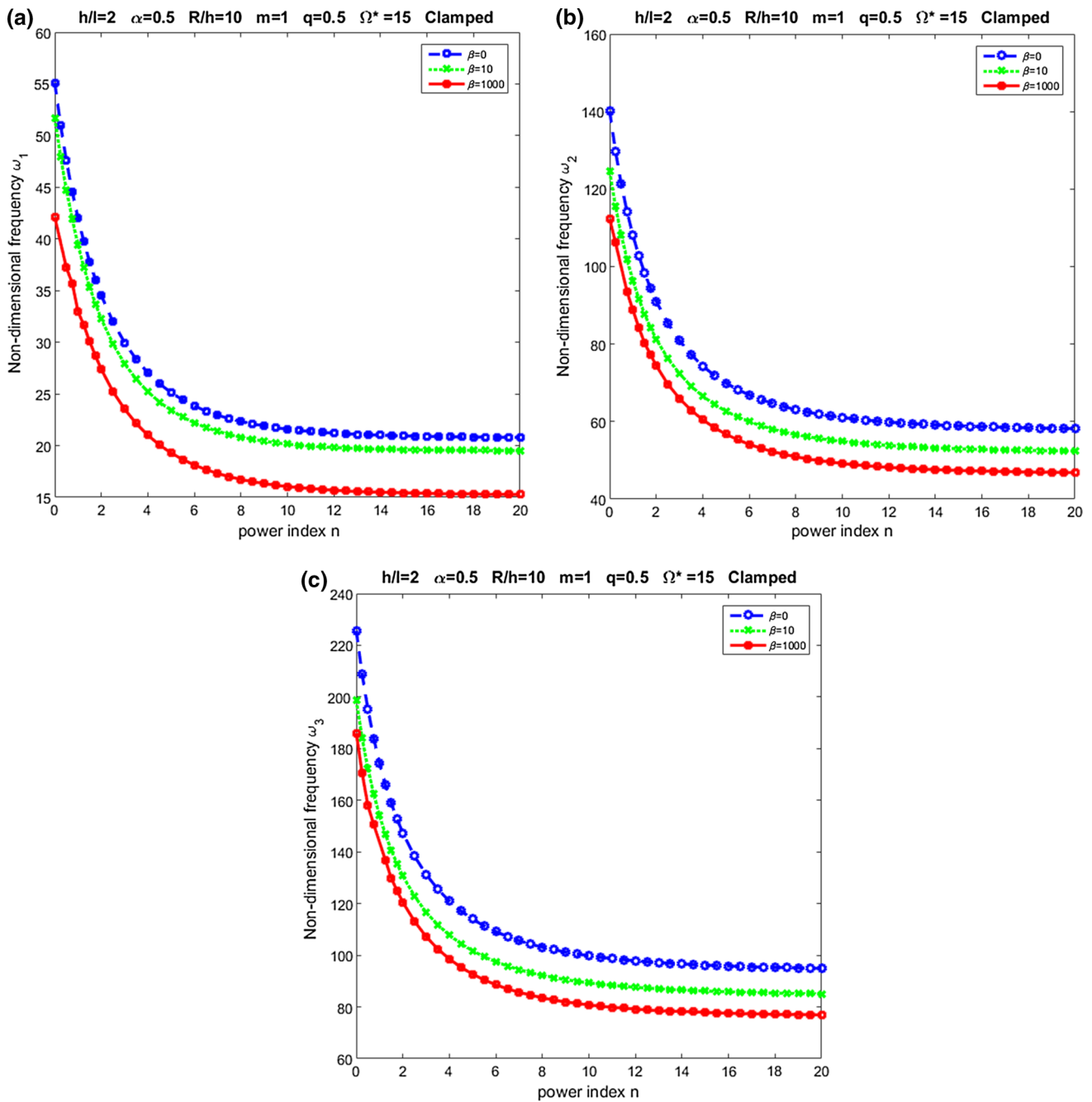
Fig. 11 A map for the two-directionality-variation of material effects on the first three non-dimensional natural frequencies of a rotating variable thickness circular microplate: **a** the first non-dimensional natural frequencies, ω_1, **b** the second non-dimensional natural frequencies, ω_2, **c** the third non-dimensional natural frequencies, ω_3

Fig. 12 The first non-dimensional natural frequencies, ω_1, of a clamped variable thickness circular microplate in terms of the non-dimensional angular velocity for different size dependencies

Fig. 13 The first non-dimensional natural frequencies, ω_1, of a hinged variable thickness circular microplate in terms of the non-dimensional angular velocity for different size dependencies

Appendix C

$$
\left[
\begin{array}{l}
(A_{11})\left(\dfrac{\partial^2 u}{\partial r^2} + \dfrac{1}{r}\dfrac{\partial u}{\partial r} - \dfrac{u}{r^2}\right) \\[6pt]
+ r\dfrac{\partial A_{11}}{\partial r}\dfrac{\partial u}{\partial r} + \dfrac{\partial A_{12}}{\partial r}u \\[6pt]
+ (B_{11})\left(\dfrac{\partial^2 \Phi}{\partial r^2} + \dfrac{1}{r}\dfrac{\partial \Phi}{\partial r} - \dfrac{\Phi}{r^2}\right) \\[6pt]
\left(r\dfrac{\partial B_{11}}{\partial r}\dfrac{\partial \Phi}{\partial r} + \dfrac{\partial B_{12}}{\partial r}\Phi\right)
\end{array}
\right]
= \left(I_1\dfrac{\partial^2 u}{\partial t^2} + I_2\dfrac{\partial^2 \Phi}{\partial t^2}\right)
$$

$$(47)$$

$$
\left[
\begin{array}{l}
\dfrac{k_s}{r}\left(A_{55}r\dfrac{\partial^2 w}{\partial r^2} + A_{55}\dfrac{\partial w}{\partial r} + \dfrac{\partial A_{55}}{\partial r}r\dfrac{\partial w}{\partial r}\right) \\[6pt]
+ \dfrac{S}{4r}\left(-\dfrac{1}{2}\dfrac{\partial^4 w}{\partial r^4} - \dfrac{1.5}{2r}\dfrac{\partial^3 w}{\partial r^3} - \left(\dfrac{1.5}{r} - \dfrac{1}{r^2}\right)\dfrac{\partial^2 w}{\partial r^2} - \left(\dfrac{1}{r^3} - \dfrac{3}{r^2}\right)\dfrac{\partial w}{\partial r}\right) \\[6pt]
- \left(\dfrac{1}{2r}\dfrac{\partial S}{\partial r}\right)\left(\dfrac{\partial^3 w}{\partial r^3} + \dfrac{1.5}{r}\dfrac{\partial^2 w}{\partial r^2} + \left(\dfrac{1.5}{r} - \dfrac{1}{r^2}\right)\dfrac{\partial w}{\partial r}\right) \\[6pt]
- \left(\dfrac{1}{2r}\dfrac{\partial^2 S}{\partial r^2}\right)\left(\dfrac{1}{2}\dfrac{\partial^2 w}{\partial r^2} + \dfrac{1.5}{r}\dfrac{\partial w}{\partial r}\right) \\[6pt]
+ \dfrac{k_s}{r}\left(A_{55}r\dfrac{\partial \Phi}{\partial r} + A_{55}\Phi + \dfrac{\partial A_{55}}{\partial r}r\Phi\right) \\[6pt]
+ \dfrac{S}{4r}\left(\dfrac{1}{2}\dfrac{\partial^3 \Phi}{\partial r^3} + \dfrac{1.5}{2r}\dfrac{\partial^2 \Phi}{\partial r^2} + \left(\dfrac{1.5}{r} - \dfrac{1}{r^2}\right)\dfrac{\partial \Phi}{\partial r} + \left(\dfrac{1}{r^3} - \dfrac{3}{r^2}\right)\Phi\right) \\[6pt]
+ \left(\dfrac{1}{2r}\dfrac{\partial S}{\partial r}\right)\left(\dfrac{\partial^2 \Phi}{\partial r^2} + \left(\dfrac{1}{r} + 1.5\right)\dfrac{\partial \Phi}{\partial r} + \left(\dfrac{1.5}{r} - \dfrac{1}{r^2}\right)\Phi\right) \\[6pt]
+ \left(\dfrac{1}{2r}\dfrac{\partial^2 S}{\partial r^2}\right)\left(\dfrac{1}{2}\dfrac{\partial \Phi}{\partial r} + \dfrac{1.5}{r}\Phi\right) + \dfrac{\partial}{r\partial r}\left(N^{Rotation}r\dfrac{\partial w}{\partial r}\right)
\end{array}
\right]
$$
$$
= I_1\dfrac{\partial^2 w}{\partial t^2}
$$

$$(48)$$

$$
\left[
\begin{array}{l}
-k_s A_{55}\dfrac{\partial w}{\partial r} + \left(-\dfrac{S}{2}\right)\left[\dfrac{1}{4}\dfrac{\partial^3 w}{\partial r^3} + \dfrac{1}{r}\dfrac{\partial^2 w}{\partial r^2} + \dfrac{1}{r^2}\dfrac{\partial w}{\partial r}\right] - \left(\dfrac{1}{4}\dfrac{\partial S}{\partial r}\right)\left(\dfrac{\partial^2 w}{\partial r^2} + \dfrac{1}{r}\dfrac{\partial w}{\partial r}\right) \\[6pt]
-k_s A_{55}\Phi + D_{11}\left(\dfrac{\partial^2 \Phi}{\partial r^2} + \dfrac{1}{r}\dfrac{\partial \Phi}{\partial r} - \dfrac{1}{r^2}\Phi\right) + \left(\dfrac{\partial D_{11}}{\partial r}\right)\left(\dfrac{\partial \Phi}{\partial r}\right) + \left(\dfrac{\partial D_{12}}{\partial r}\right)\left(\dfrac{1}{r}\Phi\right) \\[6pt]
\dfrac{1}{2}\left\{\left(\dfrac{S}{4}\right)\left(\dfrac{\partial^2 \Phi}{\partial r^2} + \dfrac{1}{r}\dfrac{\partial \Phi}{\partial r} - \dfrac{1}{r^2}\Phi\right) + \left(\dfrac{\partial S}{\partial r}\right)\left(\dfrac{\partial \Phi}{\partial r}\right) + \left(\dfrac{\partial S}{\partial r}\right)\left(\dfrac{1}{r}\Phi\right)\right\} \\[6pt]
\dfrac{1}{r}\left\{(B_{11})\left(r\dfrac{\partial^2 u}{\partial r^2} + \dfrac{\partial u}{\partial r} - \dfrac{1}{r}u\right) + \left(\dfrac{\partial B_{11}}{\partial r}\right)\left(r\dfrac{\partial u}{\partial r}\right) + \left(\dfrac{\partial B_{12}}{\partial r}\right)(u)\right\}
\end{array}
\right]
$$
$$
= I_2\dfrac{\partial^2 u}{\partial t^2} + I_3\dfrac{\partial^2 \Phi}{\partial t^2}
$$

$$(49)$$

$$
\left[\left(A_{11}\left(r\dfrac{\partial u}{\partial r}\right) + A_{12}u\right) + \left(B_{11}\left(r\dfrac{\partial \Phi}{\partial r}\right) + B_{12}\Phi\right)\right]\delta u = 0
$$
at $r = 0, R$

$$(50)$$

$$\left[\begin{array}{l} \dfrac{S}{4}\left(\dfrac{\partial^2\Phi}{\partial r^2} - \dfrac{\partial^3 w}{\partial r^3} + \dfrac{1}{r}\dfrac{\partial\Phi}{\partial r} - \dfrac{1}{r}\dfrac{\partial^2 w}{\partial r^2} - \dfrac{\Phi}{r^2} + \dfrac{1}{r^2}\dfrac{\partial w}{\partial r}\right) \\ + k_s A_{55}\left(\dfrac{\partial w}{\partial r} + \Phi\right) \\ + \dfrac{1}{4}\dfrac{\partial S}{\partial r}\left(\dfrac{\partial\Phi}{\partial r} - \dfrac{\partial^2 w}{\partial r^2} + \dfrac{1}{r}\dfrac{\partial\Phi}{\partial r} + \dfrac{1}{r} - \dfrac{\partial w}{\partial r} + \Phi\right) \end{array}\right]\delta w = 0$$

at r = 0, R

$$(51)$$

$$\left(\dfrac{S}{4}\dfrac{1}{r}\left(\left(\dfrac{\partial\Phi}{\partial r} - \dfrac{\partial^2 w}{\partial r^2}\right) - \dfrac{1}{r}\left(\Phi - \dfrac{\partial w}{\partial r}\right)\right)\right)\delta\left(\dfrac{\partial w}{\partial r}\right) = 0$$

at r = 0, R

$$(52)$$

$$\left(B_{11}\dfrac{\partial u}{\partial r} + B_{12}\dfrac{u}{r} + D_{11}\dfrac{\partial\Phi}{\partial r} + D_{12}\dfrac{\Phi}{r} + \dfrac{S}{4}\left(\left(\dfrac{\partial\Phi}{\partial r} - \dfrac{\partial^2 w}{\partial r^2}\right) - \dfrac{1}{r}\left(\Phi - \dfrac{\partial w}{\partial r}\right)\right)\right)\delta\Phi$$
$$= 0$$

at r = 0, R

$$(53)$$

Appendix D

$$\left[\begin{array}{l} (A_{11})\left(\displaystyle\sum_{k=1}^{n_i} C_{ik}^{(2)} u_k + \dfrac{1}{r_i}\sum_{k=1}^{n_i} C_{ik}^{(1)} u_k - \dfrac{u_i}{r_i^2}\right) \\ + \left(r_i\left(\displaystyle\sum_{k=1}^{n_i} C_{ik}^{(1)} A_{11}\right)\sum_{k=1}^{n_i} C_{ik}^{(1)} u_k\right)\sum_{k=1}^{n_i} + \left(\left(\displaystyle\sum_{k=1}^{n_i} C_{ik}^{(1)} A_{12}\right)(u_i)\right) \\ + (B_{11})\left(\displaystyle\sum_{k=1}^{n_i} C_{ik}^{(2)}\Phi_k + \dfrac{1}{r_i}\sum_{k=1}^{n_i} C_{ik}^{(1)}\Phi_k - \dfrac{\Phi_i}{r_i^2}\right) \\ + \left(r_i\left(\displaystyle\sum_{k=1}^{n_i} C_{ik}^{(1)} B_{11}\right)\sum_{k=1}^{n_i} C_{ik}^{(1)}\Phi_k\right) + \left(\left(\displaystyle\sum_{k=1}^{n_i} C_{ik}^{(1)} B_{12}\right)(\Phi_i)\right) \end{array}\right]$$
$$= \omega^2(I_1 u_i + I_2\Phi_i)$$

$$(54)$$

$$\left[\begin{array}{l} \left(\dfrac{S}{4r_i}\right)\left[\begin{array}{l} \dfrac{1}{2}\displaystyle\sum_{k=1}^{n_i} C_{ik}^{(3)}\Phi_k + \dfrac{1.5}{2r_i}\sum_{k=1}^{n_i} C_{ik}^{(2)}\Phi_k\left(\dfrac{1.5}{r_i} - \dfrac{1}{r_i^2}\right)\sum_{k=1}^{n_i} C_{ik}^{(1)}\Phi_k \\ + \left(\dfrac{1}{r_i^3} - \dfrac{3}{r_i^2}\right)\Phi_i - \dfrac{1}{2}\displaystyle\sum_{k=1}^{n_i} C_{ik}^{(4)} w_k - \dfrac{1.5}{2r_i}\sum_{k=1}^{n_i} C_{ik}^{(3)} w_k \\ \left(\dfrac{1.5}{r_i} - \dfrac{1}{r_i^2}\right)\displaystyle\sum_{k=1}^{n_i} C_{ik}^{(2)} w_k - \left(\dfrac{1}{r_i^3} - \dfrac{3}{r_i^2}\right)\sum_{k=1}^{n_i} C_{ik}^{(1)} w_k \end{array}\right] \\ + (k_s A_{55})\left(\displaystyle\sum_{k=1}^{n_i} C_{ik}^{(2)} w_k + \dfrac{1}{r_i}\sum_{k=1}^{n_i} C_{ik}^{(1)} w_k + \sum_{k=1}^{n_i} C_{ik}^{(1)}\Phi_k + \dfrac{\Phi_i}{r_i}\right) \\ \left(\dfrac{k_s}{r_i}\displaystyle\sum_{k=1}^{n_i} C_{ik}^{(1)} A_{55}\right)\left(r_i\sum_{k=1}^{n_i} C_{ik}^{(1)} w_k + r_i\Phi_i\right) \\ - \left(\dfrac{1}{2r_i}\displaystyle\sum_{k=1}^{n_i} C_{ik}^{(1)} S\right)\left(\sum_{k=1}^{n_i} C_{ik}^{(3)} w_k + \left(\dfrac{1.5}{r_i}\right)\sum_{k=1}^{n_i} C_{ik}^{(2)} w_k + \left(\dfrac{1.5}{r_i} - \dfrac{1}{r_i^2}\right)\sum_{k=1}^{n_i} C_{ik}^{(1)} w_k\right) \\ + \left(\left(\dfrac{1}{2r_i}\displaystyle\sum_{k=1}^{n_i} C_{ik}^{(1)} S\right)(\sum_{k=1}^{n_i} C_{ik}^{(2)}\Phi_k + \left(\dfrac{1}{r_i} + 1.5\right)\sum_{k=1}^{n_i} C_{ik}^{(1)}\Phi_k + \left(\dfrac{1.5}{r_i} - \dfrac{1}{r_i^2}\right)\Phi_i\right) \\ - \left(\left(\dfrac{1}{2r_i}\displaystyle\sum_{k=1}^{n_i} C_{ik}^{(2)} S\right)\left(\left(\dfrac{1}{2}\right)\sum_{k=1}^{n_i} C_{ik}^{(2)} w_k + \dfrac{1.5}{r_i}\sum_{k=1}^{n_i} C_{ik}^{(1)} w_k\right)\right) \\ + \left(\left(\dfrac{1}{2r_i}\displaystyle\sum_{k=1}^{n_i} C_{ik}^{(2)} S\right)\left(\left(\dfrac{1}{2}\right)\sum_{k=1}^{n_i} C_{ik}^{(1)}\Phi_k + \left(\dfrac{1.5}{r_i}\right)\Phi_i\right)\right) \\ + \dfrac{1}{r_i}\left(\displaystyle\sum_{k=1}^{n_i} C_{ik}^{(1)}\left(N^{Rotation} r\left(\sum_{k=1}^{n_i} C_{ik}^{(1)} w_k\right)\right)\right) \end{array}\right] = \omega^2 I_1 w_i$$

$$(55)$$

$$
\begin{bmatrix}
- k_s A_{55}\left(\displaystyle\sum_{k=1}^{n_i} C_{ik}^{(1)} w_k\right) - \Phi_i \\[8pt]
\left(-\dfrac{S}{2}\right)\left(\dfrac{1}{4}\displaystyle\sum_{k=1}^{n_i} C_{ik}^{(3)} w_k + \dfrac{1}{r_i}\displaystyle\sum_{k=1}^{n_i} C_{ik}^{(2)} w_k + \dfrac{1}{r_i^2}\displaystyle\sum_{k=1}^{n_i} C_{ik}^{(1)} w_k\right) \\[10pt]
- \left(\left(\dfrac{1}{4}\displaystyle\sum_{k=1}^{n_i} C_{ik}^{(1)} S\right)\left(\displaystyle\sum_{k=1}^{n_i} C_{ik}^{(2)} w_k + \dfrac{1}{r_i}\displaystyle\sum_{k=1}^{n_i} C_{ik}^{(1)} w_k\right)\right) \\[10pt]
+ \left(\dfrac{S}{4}\left(\dfrac{1}{2}\right)\right)\left(\displaystyle\sum_{k=1}^{n_i} C_{ik}^{(2)} \Phi_k + \dfrac{1}{r_i}\displaystyle\sum_{k=1}^{n_i} C_{ik}^{(1)} \Phi_k - \dfrac{\Phi_i}{r_i^2}\right) \\[10pt]
+ \left(\left(\dfrac{1}{2}\displaystyle\sum_{k=1}^{n_i} C_{ik}^{(1)} S\right)\left(\displaystyle\sum_{k=1}^{n_i} C_{ik}^{(1)} \Phi_k + \dfrac{\Phi_i}{r_i}\right)\right) \\[10pt]
+ (D_{11})\left(\displaystyle\sum_{k=1}^{n_i} C_{ik}^{(2)} \Phi_k + \dfrac{1}{r_i}\displaystyle\sum_{k=1}^{n_i} C_{ik}^{(1)} \Phi_k - \dfrac{\Phi_i}{r_i^2}\right) \\[10pt]
+ \left(\displaystyle\sum_{k=1}^{n_i} C_{ik}^{(1)} D_{11}\left(\displaystyle\sum_{k=1}^{n_i} C_{ik}^{(1)} \Phi_k\right)\right) + \left(\left(\displaystyle\sum_{k=1}^{n_i} C_{ik}^{(1)} D_{12}\right)(\Phi_i)\right) \\[10pt]
+ (B_{11})\left(\displaystyle\sum_{k=1}^{n_i} C_{ik}^{(2)} u_k + \dfrac{1}{r_i}\displaystyle\sum_{k=1}^{n_i} C_{ik}^{(1)} u_k - \dfrac{u_i}{r_i^2}\right) \\[10pt]
+ \left(\displaystyle\sum_{k=1}^{n_i} C_{ik}^{(1)} B_{11}\left(\displaystyle\sum_{k=1}^{n_i} C_{ik}^{(1)} u_k\right)\right) + \left(\displaystyle\sum_{k=1}^{n_i} C_{ik}^{(1)} B_{12}(u_i)\right)
\end{bmatrix}
$$
$$
= \omega^2 (I_3 \Phi_i + I_2 u_i) \tag{56}
$$

References

Akgöz B, Civalek Ö (2013) Free vibration analysis of axially functionally graded tapered Bernoulli–Euler microbeams based on the modified couple stress theory. Compos Struct 98:314–322. doi:10.1016/j.compstruct.2012.11.020

Alinaghizadeh F, Shariati M (2015) Static analysis of variable thickness two-directional functionally graded annular sector plates fully or partially resting on elastic foundations by the GDQ method. J Braz Soc Mech Sci Eng. doi:10.1007/s40430-015-0427-0

Alinaghizadeh F, Shariati M (2016) Geometrically non-linear bending analysis of thick two-directional functionally graded annular sector and rectangular plates with variable thickness resting on non-linear elastic foundation. Compos Part B Eng 86:61–83. doi:10.1016/j.compositesb.2015.05.010

Alipour MM, Shariyat M (2013) Semianalytical solution for buckling analysis of variable thickness two-directional functionally graded circular plates with nonuniform elastic foundations. J Eng Mech 139:664–676. doi:10.1061/(ASCE)EM.1943-7889.0000522

Alshorbagy AE, Eltaher MA, Mahmoud FF (2011) Free vibration characteristics of a functionally graded beam by finite element method. Appl Math Model 35:412–425. doi:10.1016/j.apm.2010.07.006

Anjomshoa A (2013) Application of Ritz functions in buckling analysis of embedded orthotropic circular and elliptical micro/nano-plates based on nonlocal elasticity theory. Meccanica 48:1337–1353. doi:10.1007/s11012-012-9670-y

Ansari R, Gholami R, Faghih Shojaei M, Mohammadi V, Sahmani S (2015) Bending, buckling and free vibration analysis of size-dependent functionally graded circular/annular microplates based on the modified strain gradient elasticity theory. Eur J Mech A/Solids 49:251–267. doi:10.1016/j.euromechsol.2014.07.014

Aydogdu M, Taskin V (2007) Free vibration analysis of functionally graded beams with simply supported edges. Mater Des 28:1651–1656. doi:10.1016/j.matdes.2006.02.007

Bauer HF, Eidel W (2007) Transverse vibration and stability of spinning circular plates of constant thickness and different boundary conditions. J Sound Vib 300:877–895. doi:10.1016/j.jsv.2006.09.001

Bedroud M, Hosseini-Hashemi S, Nazemnezhad R (2013) Buckling of circular/annular Mindlin nanoplates via nonlocal elasticity. Acta Mech 224:2663–2676. doi:10.1007/s00707-013-0891-5

Chaht FL, Kaci A, Sid M, Houari A, Tounsi A, Bég OA et al (2015) Bending and buckling analyses of functionally graded material (FGM) size-dependent nanoscale beams including the thickness stretching effect. Steel Compos Struct 2:425–442. doi:10.12989/scs.2015.18.2.425

Duan WH, Wang CM (2007) Exact solutions for axisymmetric bending of micro/nanoscale circular plates based on nonlocal plate theory. Nanotechnology 18:385704. doi:10.1088/0957-4484/18/38/385704

Ebrahimi F, Ghadiri M, Salari E, Hoseini SAH, Shaghaghi GR (2015) Application of the differential transformation method for non-local vibration analysis of functionally graded nanobeams. J Mech Sci Technol 29:1207–1215. doi:10.1007/s12206-015-0234-7

Eshraghi I, Dag S, Soltani N (2016) Bending and free vibrations of functionally graded annular and circular micro-plates under thermal loading. Compos Struct 137:196–207. doi:10.1016/j.compstruct.2015.11.024

Farajpour A, Shahidi AR, Mohammadi M, Mahzoon M (2012) Buckling of orthotropic micro/nanoscale plates under linearly varying in-plane load via nonlocal continuum mechanics. Compos Struct 94:1605–1615. doi:10.1016/j.compstruct.2011.12.032

Ghadiri M, Hosseini M (2014) Vibration analysis of a laminated composite beam with non-ideal boundary conditions. Int J Basic Sci Appl Res 1:15–18

Ghadiri M, Shafiei N (2015) Nonlinear bending vibration of a rotating nanobeam based on nonlocal Eringen's theory using differential quadrature method. Microsyst Technol. doi:10.1007/s00542-015-2662-9

Ghadiri M, Shafiei N (2016a) Vibration analysis of rotating functionally graded Timoshenko microbeam based on modified couple stress theory under different temperature distributions. Acta Astronaut 121:221–240. doi:10.1016/j.actaastro.2016.01.003

Ghadiri M, Shafiei N (2016b) Vibration analysis of a nano-turbine blade based on Eringen nonlocal elasticity applying the differential quadrature method. J Vib Control. doi:10.1177/1077546315627723

Ghadiri M, Malekzadeh K, Ghasemi FA (2015) Free vibration of an axially preloaded laminated composite beam carrying a spring-mass-damper system with a non-ideal support. Jordan J Mech Ind Eng 9:195–207

Ghadiri M, Shafiei N, Safarpour H (2016) Influence of surface effects on vibration behavior of a rotary functionally graded nanobeam based on Eringen's nonlocal elasticity. Microsyst Technol. doi:10.1007/s00542-016-2822-6

Gholami R, Ansari R, Darvizeh A, Sahmani S (2015) Axial buckling and dynamic stability of functionally graded microshells based on the modified couple stress theory. Int J Struct Stab Dyn 15:1450070. doi:10.1142/S0219455414500709

Gholami R, Darvizeh A, Ansari R, Sadeghi F (2016) Vibration and buckling of first-order shear deformable circular cylindrical

micro-/nano-shells based on Mindlin's strain gradient elasticity theory. Eur J Mech A/Solids 58:76–88. doi:10.1016/j.euromechsol.2016.01.014

Huang Y, Li XF (2010) A new approach for free vibration of axially functionally graded beams with non-uniform cross-section. J Sound Vib 329:2291–2303. doi:10.1016/j.jsv.2009.12.029

Huang Y, Yang LE, Luo QZ (2013) Free vibration of axially functionally graded Timoshenko beams with non-uniform cross-section. Compos Part B Eng 45:1493–1498. doi:10.1016/j.compositesb.2012.09.015

Irie T, Yamada G, Aomura S (1980) Natural frequencies of Mindlin circular plates. J Appl Mech 47:652–655

Jabbari M, Farzaneh Joubaneh E, Mojahedin A (2014) Thermal buckling analysis of porous circular plate with piezoelectric actuators based on first order shear deformation theory. Int J Mech Sci 83:57–64. doi:10.1016/j.ijmecsci.2014.03.024

Jin TL, Ha NS, Goo NS (2014) A study of the thermal buckling behavior of a circular aluminum plate using the digital image correlation technique and finite element analysis. Thin Walled Struct 77:187–197. doi:10.1016/j.tws.2013.10.012

Kadkhodayan M, Golmakani ME (2014) Non-linear bending analysis of shear deformable functionally graded rotating disk. Int J Non Linear Mech 58:41–56. doi:10.1016/j.ijnonlinmec.2013.08.007

Ke LL, Yang J, Kitipornchai S, Bradford MA (2012) Bending, buckling and vibration of size-dependent functionally graded annular microplates. Compos Struct 94:3250–3257. doi:10.1016/j.compstruct.2012.04.037

Khalili SMR, Jafari AA, Eftekhari SA (2010) A mixed Ritz-DQ method for forced vibration of functionally graded beams carrying moving loads. Compos Struct 92:2497–2511. doi:10.1016/j.compstruct.2010.02.012

Leissa AW (1969) Vibration of plates. Defence technical information center document. Accession Number: ADA307623

Liew KM, Han J-B, Xiao ZM (1997) Vibration analysis of circular Mindlin plates using the differential quadrature method. J Sound Vib 205:617–630

Ma LS, Wang TJ (2003) Nonlinear bending and post-buckling of a functionally graded circular plate under mechanical and thermal loadings. Int J Solids Struct 40:3311–3330. doi:10.1016/S0020-7683(03)00118-5

Mehri M, Asadi H, Wang Q (2016) Buckling and vibration analysis of a pressurized CNT reinforced functionally graded truncated conical shell under an axial compression using HDQ method. Comput Methods Appl Mech Eng 303:75–100. doi:10.1016/j.cma.2016.01.017

Neves AMA, Ferreira AJM, Carrera E, Roque CMC, Cinefra M, Jorge RMN et al (2012a) A quasi-3D sinusoidal shear deformation theory for the static and free vibration analysis of functionally graded plates. Compos Part B Eng 43:711–725. doi:10.1016/j.compositesb.2011.08.009

Neves AMA, Ferreira AJM, Carrera E, Cinefra M, Roque CMC, Jorge RMN et al (2012b) A quasi-3D hyperbolic shear deformation theory for the static and free vibration analysis of functionally graded plates. Compos Struct 94:1814–1825. doi:10.1016/j.compstruct.2011.12.005

Neves AMA, Ferreira AJM, Carrera E, Cinefra M, Roque CMC, Jorge RMN et al (2013) Free vibration analysis of functionally graded shells by a higher-order shear deformation theory and radial basis functions collocation, accounting for through-the-thickness deformations. Eur J Mech A/Solids 37:24–34. doi:10.1016/j.euromechsol.2012.05.005

Özakça M, Tayşi N, Kolcu F (2003) Buckling analysis and shape optimization of elastic variable thickness circular and annular plates-I. Finite element formulation. Eng Struct 25:181–192. doi:10.1016/S0141-0296(02)00133-5

Pradhan KK, Chakraverty S (2013) Free vibration of Euler and Timoshenko functionally graded beams by Rayleigh–Ritz method. Compos Part B Eng 51:175–184. doi:10.1016/j.compositesb.2013.02.027

Reddy JN, Berry J (2012) Nonlinear theories of axisymmetric bending of functionally graded circular plates with modified couple stress. Compos Struct 94:3664–3668. doi:10.1016/j.compstruct.2012.04.019

Salamat-Talab M, Nateghi A, Torabi J (2012) Static and dynamic analysis of third-order shear deformation FG micro beam based on modified couple stress theory. Int J Mech Sci 57:63–73. doi:10.1016/j.ijmecsci.2012.02.004

Satouri S (2015) Natural frequency analysis of 2D-FGM sectorial plate with variable thickness resting on elastic foundation using 2D-DQM. Int J Appl Mech 7:1550030. doi:10.1142/S1758825115500301

Shafiei N, Mousavi A, Ghadiri M (2016a) Y13Vibration behavior of a rotating non-uniform FG microbeam based on the modified couple stress theory and GDQEM. Compos Struct. doi:10.1016/j.compstruct.2016.04.024

Shafiei N, Kazemi M, Ghadiri M (2016b) On size-dependent vibration of rotary axially functionally graded microbeam. Int J Eng Sci 101:29–44. doi:10.1016/j.ijengsci.2015.12.008

Shafiei N, Kazemi M, Ghadiri M (2016c) Comparison of modeling of the rotating tapered axially functionally graded Timoshenko and Euler–Bernoulli microbeams. Elsevier. doi:10.1016/j.physe.2016.04.011

Shafiei N, Kazemi M, Ghadiri M (2016d) Nonlinear vibration of axially functionally graded tapered microbeams. Int J Eng Sci 102:12–26. doi:10.1016/j.ijengsci.2016.02.007

Shahba A, Rajasekaran S (2012) Free vibration and stability of tapered Euler–Bernoulli beams made of axially functionally graded materials. Appl Math Model 36:3094–3111. doi:10.1016/j.apm.2011.09.073

Shahba A, Attarnejad R, Marvi MT, Hajilar S (2011) Free vibration and stability analysis of axially functionally graded tapered Timoshenko beams with classical and non-classical boundary conditions. Compos Part B Eng 42:801–808. doi:10.1016/j.compositesb.2011.01.017

Shariyat M, Alipour MM (2013) A power series solution for vibration and complex modal stress analyses of variable thickness viscoelastic two-directional FGM circular plates on elastic foundations. Appl Math Model 37:3063–3076. doi:10.1016/j.apm.2012.07.037

Shariyat M, Jafari AA, Alipour MM (2013) Investigation of the thickness variability and material heterogeneity effects on free vibration of the viscoelastic circular plates. Acta Mech Solida Sin 26:83–98. doi:10.1016/S0894-9166(13)60009-9

Shu C (2012) Differential quadrature and its application in engineering. Springer, London

Şimşek M (2010a) Vibration analysis of a functionally graded beam under a moving mass by using different beam theories. Compos Struct 92:904–917. doi:10.1016/j.compstruct.2009.09.030

Şimşek M (2010b) Non-linear vibration analysis of a functionally graded Timoshenko beam under action of a moving harmonic load. Compos Struct 92:2532–2546. doi:10.1016/j.compstruct.2010.02.008

Şimşek M (2012) Nonlocal effects in the free longitudinal vibration of axially functionally graded tapered nanorods. Comput Mater Sci 61:257–265. doi:10.1016/j.commatsci.2012.04.001

Şimşek M, Kocatürk T (2009) Free and forced vibration of a functionally graded beam subjected to a concentrated moving harmonic load. Compos Struct 90:465–473. doi:10.1016/j.compstruct.2009.04.024

Şimşek M, Reddy JN (2013) Bending and vibration of functionally graded microbeams using a new higher order beam theory and

the modified couple stress theory. Int J Eng Sci 64:37–53. doi:10.1016/j.ijengsci.2012.12.002

Şimşek M, Kocatürk T, Akbaş ŞD (2012) Dynamic behavior of an axially functionally graded beam under action of a moving harmonic load. Compos Struct 94:2358–2364. doi:10.1016/j.compstruct.2012.03.020

Tsiatas GC, Yiotis AJ (2014) Size effect on the static, dynamic and buckling analysis of orthotropic Kirchhoff-type skew micro-plates based on a modified couple stress theory: comparison with the nonlocal elasticity theory. Acta Mech 226:1267–1281. doi:10.1007/s00707-014-1249-3

Van Dung D, Hoa LK (2013) Nonlinear buckling and post-buckling analysis of eccentrically stiffened functionally graded circular cylindrical shells under external pressure. Thin Walled Struct 63:117–124. doi:10.1016/j.tws.2012.09.010

Wang CM, Zhang YY, Ramesh SS, Kitipornchai S (2006) Buckling analysis of micro- and nano-rods/tubes based on nonlocal Timoshenko beam theory. J Phys D Appl Phys 39:3904–3909. doi:10.1088/0022-3727/39/17/029

Wei D, Liu Y, Xiang Z (2012) An analytical method for free vibration analysis of functionally graded beams with edge cracks. J Sound Vib 331:1686–1700. doi:10.1016/j.jsv.2011.11.020

Wu T, Wang Y, Liu G (2002) Free vibration analysis of circular plates using generalized differential quadrature rule. Comput Methods Appl Mech Eng 191:5365–5380. doi:10.1016/S0045-7825(02)00463-2

Yalcin HS, Arikoglu A, Ozkol I (2009) Free vibration analysis of circular plates by differential transformation method. Appl Math Comput 212:377–386. doi:10.1016/j.amc.2009.02.032